Materials and Design 175 (2019) 107813

Contents lists available at ScienceDirect

Materials and Design

journal homepage: www.elsevier.com/locate/matdes

Harnessing multi-layered soil to design seismic metamaterials with ultralow frequency band gaps

Yanyu Chen [a], Feng Qian [b], Fabrizio Scarpa [c], Lei Zuo [b,*], Xiaoying Zhuang [d,e,**]

[a] Department of Mechanical Engineering, University of Louisville, Louisville, KY 40292, USA
[b] Department of Mechanical Engineering, Virginia Tech, Blacksburg, VA 24061, USA
[c] Bristol Composites Institute (ACCIS) and Dynamics and Control Research Group (DCRG), University of Bristol, BS8 1TR Bristol, UK
[d] Department of Geotechnical Engineering, College of Civil Engineering, Tongji University, Shanghai 200092, PR China
[e] State Key Laboratory for Disaster Reduction in Civil Engineering, Tongji University, Shanghai 200092, PR China

HIGHLIGHTS

- Lab scale experiments were conducted to understand elastic wave propagation in seismic metamaterials.
- Finite element models for wave propagation analysis were validated against the experiments.
- Multi-layered seismic metamaterials can attenuate surface waves by confining wave energy.
- Broadband cut-off band gaps up to 7.2 Hz were predicted in the multilayered seismic metamaterials.

GRAPHICAL ABSTRACT

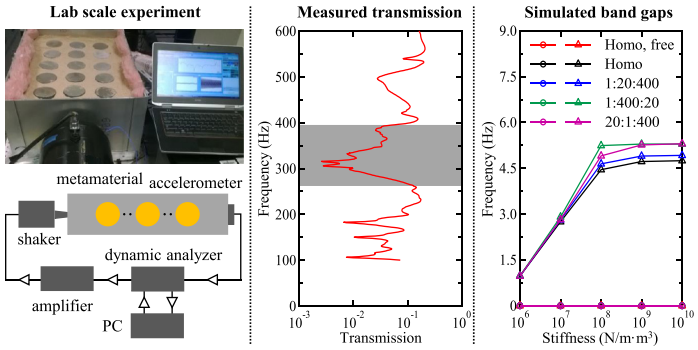

ARTICLE INFO

Article history:
Received 5 March 2019
Received in revised form 9 April 2019
Accepted 21 April 2019
Available online 23 April 2019

Keywords:
Seismic metamaterial
Vibration
Multilayered soil
Wave propagation
Phononic
Band gaps

ABSTRACT

Phononic metamaterials are capable of manipulating mechanical wave propagation in applications ranging from nanoscale heat transfer to noise and vibration mitigation. The design of phononic metamaterials to control low-frequency vibrations, such as those induced by ground transportation and low-amplitude seismic waves, however, remains a challenge. Here we propose a new design methodology to generate seismic metamaterials that can attenuate surface waves below 10 Hz. Our design concept evolves around the engineering of the multi-layered soil, the use of conventional construction materials, and operational construction constraints. The proposed seismic metamaterials are constructed by periodically varying concrete piles in the host multi-layered soil. We first validate the design concept and the numerical models by performing a lab-scale experiment on the low-amplitude surface wave propagation in a finite-size seismic metamaterial. To the best of the Authors' knowledge, this is one of the few attempts made to date to experimentally understand the vibration mitigation capability of seismic metamaterials. We then numerically demonstrate that the multi-layered seismic metamaterials can attenuate surface waves over a wide frequency range, with the incident wave energy being confined within the softest layer of the shallow layered seismic metamaterials. In addition to the localized wave energy distribution, deep layered seismic metamaterials exhibit broadband cut-off band gaps up to 7.2 Hz due to the strongly imposed constraint between piles and surrounding soil. Furthermore, these cut-off band gaps strongly depend on the constraint between the piles and the bottom layer of the soil and hence can be tuned by tailoring

* Corresponding author.
** Correspondence to: X. Zhuang, Department of Geotechnical Engineering, College of Civil Engineering, Tongji University, Shanghai 200092, PR China.
E-mail addresses: leizuo@vt.edu (L. Zuo), xiaoyingzhuang@tongji.edu.cn (X. Zhuang).

https://doi.org/10.1016/j.matdes.2019.107813

the foundation stiffness. We also evidence the possibility to create constant wave band gaps by introducing hollow concrete piles with pile volume fraction <10% in the deep layered seismic metamaterials. The findings reported here open new avenues to protect engineering structures from low-frequency seismic vibrations.

1. Introduction

Undesired mechanical vibrations arising from ground transportation, use of machinery in construction sites and low-amplitude earthquakes not only cause disruptions, but also have adverse health, social, and economic impacts. A rich low-frequency dynamics environment is abundant in metropolitan areas with high-density population and high capacity of motorways and railways. As such, serious potential health effects are induced due to the increased noise and vibration. For example, early small-scale laboratory investigation has shown that a combination of noise and vibration induced by heavy road traffic can cause significant sleep disturbances [1]. In addition to these apparent disturbances, ground vibrations and low amplitude seismic waves affect the proper operation of highly sensitive instruments, which are often employed in scientific research laboratories and high-tech industries. Technical and environmental challenges are now particularly addressed in the new built environment to tackle noise and ground motion. Many vibration mitigation approaches have been proposed to mitigate or eliminate the effects of vibration on infrastructures and facilities. Among those, passive vibration isolation solutions have attracted a significant amount of interest. For example, open or filled trenches [2–4] and large volume concrete piles [5–9] are often employed as wave barriers in engineering practice. Open/filled trenches are designed to interrupt the wave propagation path and hence mitigate mechanical vibrations for shallow structures. Concrete piles have been recently exploited as a new vibration mitigation approach for deep structures since they are immune to the influence of high groundwater level and can also enhance the ground load capacity. Experimental studies have validated the effectiveness of pile barriers to reduce structural vibrations subjected to ground vibration [9]. Though these vibration mitigation approaches have been widely adopted in current engineering practice, a quantitative understanding of the effectiveness at target frequency ranges is still not completely reached yet.

Recent studies have shown that phononic metamaterials, which are rationally designed multiscale material systems, can manipulate propagating mechanical waves, and therefore offer new solutions to effectively control noise and vibrations [10–19]. The intrinsic periodic array nature of phononic metamaterials leads to the modification of phonon dispersion relations and the possibility of tailoring group velocities. One of the remarkable features in phonon dispersion relations is the existence of omnidirectional band gaps, i.e. frequency ranges in which the propagation of phonons is prohibited, irrespective of the direction of the incident waves. Seismic metamaterials have been developed to make use of omnidirectional band gap properties, for minimizing undesired ground vibrations and low-amplitude seismic waves [20–28]. For example, two-dimensional (2D) periodic composite systems, akin to 2D phononic crystals, have been designed and been numerically shown to have the capability to attenuate ground vibrations for civil infrastructures [29–34]. In parallel, a lab-scale experiment has been conducted to test the vibration mitigation ability of a scaled periodic foundation [35]. More recently, a large-scale seismic metamaterial composed of a periodic array of cylindrical boreholes in soil has been developed to control low amplitude surface waves [36]. In situ experiment has demonstrated that the proposed seismic metamaterial can effectively reflect incoming waves at 50 Hz, and this has also been validated by the numerical simulations. The frequency ranges of most ground transportation vibrations and seismic waves are typically below 10 Hz; this requires the use of components with large sizes and, therefore, makes the above periodic structures concepts very difficult to apply. To overcome this limitation, locally resonant seismic metamaterials with low-frequency band gaps have been proposed [22,25,37,38]. Both numerical modeling and lab-scale experiments have demonstrated that artificially designed resonator geometries can be employed to control low-frequency vibrations. Nonetheless, these resonators typically have complex architectures and consist of multiple materials systems. Complexity and the assembly of heterogeneous materials could pose a significant challenge to build an effective seismic metamaterial at large scale in a construction site.

Here we propose a methodology to create a new class of seismic metamaterials to mitigate low-frequency surface waves (<10 Hz) occurring in ground transportation-induced low amplitude vibrations and low-amplitude seismic waves. Our design builds upon the use of multi-layered soil with different mechanical properties and takes into consideration the availability of conventional construction materials and the presence of build constraints. We first validate our design methodology by performing a lab-scale experiment on surface wave transmission in a homogenous seismic metamaterial. We then perform numerical simulations to understand the effect of soil layering on the mitigation of surface wave transmission. We also describe how the proposed design methodology could be used to create cost-effective seismic metamaterials. This work stands out as a practical design combining the usage of conventional construction materials with the broadband and ultralow frequency vibration mitigation capability.

2. Materials and methods

2.1. Multilayered seismic metamaterial design

Our design is inspired by the observation that multiple layers with different mechanical properties exist in the soils [39–41] (Fig. 1(a)). We also consider the availability of conventional construction materials and real construction/building constraints; circular concrete piles are therefore considered in this work (Fig. 1(b)). By periodically drilling circular concrete piles into the layered soil, we obtain a new type of seismic metamaterials with a square symmetry. Depending on the pile height, the unit cells for Bloch wave analysis can be categorized into three cases (Fig. 1(c)) [42,43], which are: 1) a shallow pile within homogeneous soil; 2) a deep pile within three layers of soil, and 3) a deep pile within four layers of soil and constrained by the bottom layer. The geometric description of these unit cells is summarized in the caption of Fig. 1.

2.2. Numerical simulations of the phononic dispersion relation and wave transmission

Here we consider in-plane surface wave propagation in the proposed three-dimensional (3D) seismic metamaterials as given by [44]:

$$-\rho\omega^2\mathbf{u} = \frac{E}{2(1+\nu)}\nabla^2\mathbf{u} + \frac{E}{2(1+\nu)(1-2\nu)}\nabla(\nabla\cdot\mathbf{u}) \quad (1)$$

where $\mathbf{u}$ is the displacement vector and ω is the angular frequency. E, ν, and ρ are the Young's modulus, the Poisson's ratio, and the density of the constituent materials, respectively. Here, the concrete piles have a modulus of 40 GPa, Poisson's ratio of 0.2, and a density of 2500 kg/m^3 [45]. Soil is a complex material with a wide range of mechanical

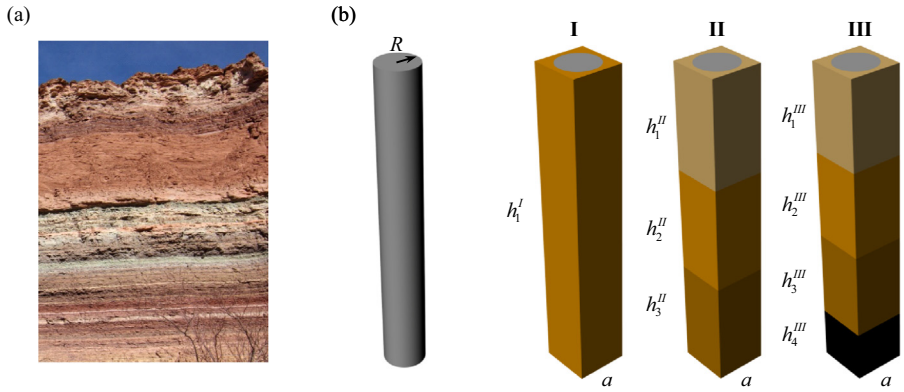

Fig. 1. Schematics of the proposed seismic metamaterials with a periodic array of concrete piles drilled in multilayered soil. (a) Layered characteristic of the soil. (b) A typical circular concrete pile, where R is the radius of the pile. (c) Three types of unit cells for Bloch wave analysis. Here h_j^i is the height of the jth layer of the unit cell type i; a is the lattice constant of the seismic metamaterials. Type I is the seismic metamaterial with homogeneous soil; type II with three layers of soil, and type III has four layers of soil and constrained by the bottom layer. For the unit cell with multi-layered soil, the modulus ratio from the top layer to the bottom layer is defined as $E_1 : E_2 : E_3$.

properties [46]. Here we assume that each layer of soil has an identical Poisson's ratio of 0.3 and a density of 1800 kg/m^3. The modulus ratio from the top layer to the bottom layer is defined as $E_1 : E_2 : E_3$.

The phononic dispersion relations are constructed by performing eigenfrequency analyses to a unit cell. The Floquet-Bloch periodic boundary conditions are applied at the boundaries of the unit cell such that [47]:

$$\mathbf{u}_i(\mathbf{r}+\mathbf{a}) = e^{i\mathbf{k}\cdot\mathbf{a}}\mathbf{u}_i(\mathbf{r}) \tag{2}$$

where $\mathbf{r}$ is the location vector that connects corresponding points on the unit cell's boundary, $\mathbf{a}$ is the lattice translation vector, and $\mathbf{k}$ is the wave vector. The governing Eq. (1) combined with the boundary condition (2) leads to the standard eigenvalue problem:

$$(\mathbf{K}-\omega^2\mathbf{M})\mathbf{U} = 0 \tag{3}$$

where $\mathbf{U}$ is the assembled displacement vector, and $\mathbf{K}$ and $\mathbf{M}$ are the global stiffness and mass matrices assembled using standard finite element analysis procedure. The unit cell is discretized using 4-node tetrahedral elements. In our simulations, we have used a discretization of 10 elements for the minimum wavelength [48,49]. Eq. (3) is then numerically solved by imposing the two components of the wave vectors and hence calculates the corresponding eigenfrequencies. The phonon dispersion relations are obtained by scanning the wave vectors in the first irreducible Brillouin zone of the square lattice [50].

The dynamic response of the proposed seismic metamaterials under both longitudinal and transverse wave excitations was calculated by performing frequency domain analyses. Perfectly matched layers (PMLs) are applied at the two ends of the homogeneous parts to prevent reflections by scattering waves from the domain boundaries [51,52]. The PMLs have the same dimensions as the unit cell. Homogenous parts having the same width and height, but a length twice that of the unit cell are positioned between the seismic metamaterials and the PMLs themselves. Soil properties are assigned to both PMLs and the homogeneous parts. To model the elastic wave propagation in the seismic metamaterials, a low-amplitude harmonic displacement is applied to the surface between the PML and the homogeneous part on the left-hand side. Here we have again used a discretization of 10 elements for minimum wavelength. It should be pointed out that the artificially applied PMLs could lead to unphysical wave modes such as radiative regions, leading to the misrepresentations of the wave attenuation properties of the proposed seismic metamaterials [53]. In this sense, a detailed sound cone analysis of the dispersion relations should be performed to identify real propagating surface waves, bulk modes, and leaky surface modes. The simulations in this work are however focused on bulk wave attenuation at the lowest frequency range, i.e., the cut-off band gaps, while most of the radiative regions lie in the higher frequency bands. Therefore, a detailed sound cone analysis is out of the scope of current theme pursued in this paper.

2.3. Lab-scale experimental setup and low-amplitude wave transmission testing

Experiments were performed on a finite-size seismic metamaterial composed of sand and 3 × 5 steel cylinders with a diameter of 7.7 cm. The cylinders are arranged with a square lattice symmetry and the lattice constant is set as 10 cm and the depth of the seismic metamaterial is 20 cm. The steel cylinder has a modulus of 210 GPa, Poisson's ratio of 0.3, and a density of 7850 kg/m^3. The sand has a modulus of 6 MPa, Poisson's ratio of 0.3, and a density of 1600 kg/m^3 [46]. The experimental setup is shown in Fig. 2(a) and sketched in Fig. 2(b). The sample is housed in a steel container with a soft cushion at two sides reducing wave reflection. An electromagnetic shaker (SENTEK VT-1000, Sentek Dynamics) is connected to the movable plate at one end of the container to provide excitation by simulating ground motion.

The excitation signal is sinusoidal with a sweeping frequency between 100 Hz and 600 Hz, and constant amplitude. A Spider 80× dynamic analyzer (Crystal Instruments) is used to control and monitor the experiment. The input signal to the shaker is generated by the dynamic analyzer and then amplified by a power amplifier (HAS 4051, NF Corporation). Two accelerometers have been used to capture the input and output acceleration signals (PCB 356A17). One accelerometer is directly attached to the shaker and the other is mounted on the far end plate of the sample. The transfer function from the input to the output has been then computed.

3. Results and discussions

3.1. Experimental validation of numerical models

To validate the proposed seismic metamaterial design concept, we have performed a lab-scale experiment on the elastic bulk wave transmission and calculated the corresponding phononic dispersion relation. As shown in Fig. 2(c), five omnidirectional band gaps are predicted by our numerical simulations. Destructive interferences are responsible for the formation of these band gaps, as this seismic metamaterial configuration is akin to a conventional 2D phononic crystal. The largest partial wave band gap along the **ΓX** direction (gray shaded area) lies between 261 Hz and 393 Hz, which closely match the attenuation zone in the measured transmission spectrum (Fig. 2(d)). This direct comparison indicates that our numerical modeling approach can

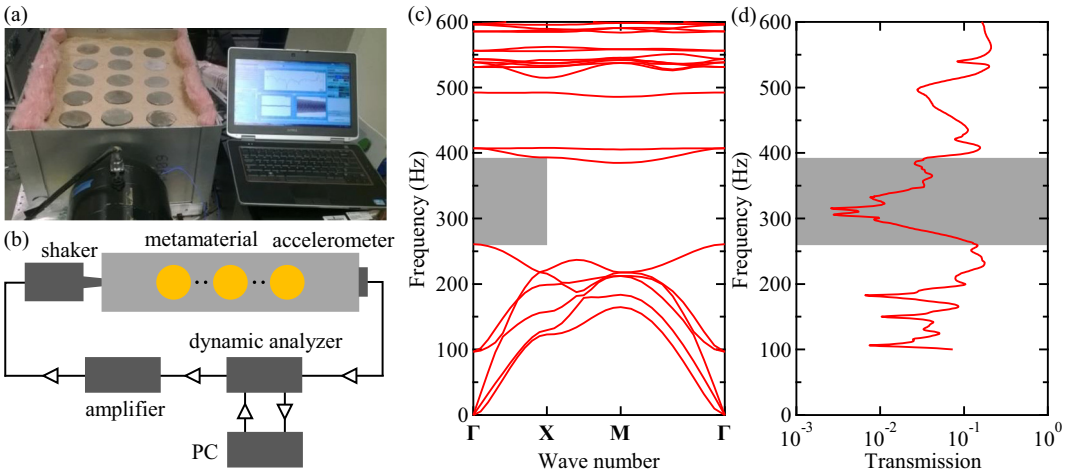

Fig. 2. The lab-scale experiment setup and validation of seismic metamaterial with homogeneous soil (Type I) for vibration mitigation. (a)-(b) Experimental setup and schematic for the surface wave transmission testing. (c) Numerically simulated phononic dispersion relation. (d) Measured transmission spectrum. Here $h_1^I = 20$cm, $a = 10$cm, and $R = 3.85$cm. The gray shaded areas in (c) and (d) indicates the partial band gap.

predict well the wave attenuation phenomenon in the proposed seismic metamaterial design concept. In addition to the seismic metamaterials with a square lattice symmetry studied here, we have also numerically and experimentally investigated the wave attenuation capability of seismic metamaterials with a triangular lattice symmetry. Our results indicate that with the same pile dimensions and lattice constants, the triangular metamaterial provides a relative larger and higher frequency band gaps, however it requires a higher volume fraction of piles. Since the objective of this work is to propose a seismic metamaterial configuration with low-frequency band gaps and low costs, we have limited our experimental and numerical work to the configuration with a square lattice symmetry.

Although the lab-scale experiment demonstrates the vibration mitigation capability of the proposed seismic metamaterial, it is, however, impracticable to use steel piles with such a large volume fraction (~50%) because of cost-effectiveness and construction constraints. Our previous work, however, implies that a large volume fraction and a mechanical impedance mismatch are essential to generate wide omnidirectional band gaps [54]. These conflicting design requirements motive us to search for new methodologies to improve the current metamaterial configuration, while also considering the availability of conventional construction materials, their cost-effectiveness, and manufacturing limitations. In the following, we will systematically investigate the wave attenuation capability of the improved seismic metamaterials composed of multi-layered soil and conventional circular concrete piles.

3.2. Multilayered seismic metamaterials for vibration mitigation

Having shown that the proposed seismic metamaterials can attenuate surface waves, we now proceed to numerically examine the effect of a layered configuration of the soil on the wave propagation. Here we limit the height of the proposed seismic metamaterials to 6 m and 18 m, which are shallow for large scale structures, but still applicable to most infrastructures such as foundations of oil tanks and nuclear power plants. To differentiate the effect of pile height and the associated layered feature, we definite the seismic metamaterials with a height of 6 m as shallow seismic metamaterials, while the ones with a height of 18 m as deep seismic metamaterials. We start with shallow seismic metamaterials with a lattice constant of 3 m. The periodically arranged concrete piles have a height of 6 m and a radius of 1.2 m, leading to a unit cell with 50% volume fraction of concrete pile. The unit cell consists of three different layers of soil with a stiffness contrast of $E_1 : E_2 : E_3 = 1 : 20 : 400$, where the second layer of soil has a Young's modulus of 20 MPa. Though this sharp stiffness contrast among different soil layers is uncommon in engineering practice, this specific soil stratification can be realized by replacing the soil with the desired mechanical properties. For the purpose of a fair comparison, the unit cell with a homogenous soil is also evaluated. An omnidirectional band gap ranging between 26 Hz and 29 Hz is observed in the dispersion relation of the homogenous seismic metamaterial (Fig. 3(a)). The global vibrational modes at the high symmetry points *A* and *B* indicate that destructive interferences (Bragg scattering) are responsible for the wave attenuation. The incoming wave with a frequency inside this band gap will be reflected by the homogeneous seismic metamaterial (Fig. 3(c)). Though an omnidirectional band gap exists, the frequency range and width are still insufficient for ground transportation induced vibrations and low amplitude seismic waves. In contrast to the homogenous seismic metamaterial, the layered seismic metamaterial displays two partial band gaps along the **XM** direction (Fig. 3(b)). These band gaps all lie below 10 Hz, which is of particular interest for the low-frequency vibration control. The vibrational modes at the high symmetry points *C* and *D* are different from those in the homogenous seismic metamaterials. Instead of reflecting the wave energy elsewhere, the layered seismic metamaterials appear to trap the wave energy, while no vibration can be observed in other layers (Fig. 3(d)). This vibration energy distribution in the layered seismic metamaterial is expected since the partial band gaps are bounded by flat bands with a zero-group velocity. Physically, these vibrational modes correspond to local resonances, which intrinsically arise from the multi-layered characteristic of the soil.

We then study the surface wave propagation in the relatively deep layered seismic metamaterial. Here the height of the seismic metamaterial is increased to 18 m while the lattice constant and pile radius are the same as those of the above shallow seismic metamaterial. The unit cell has four layers of soil, where the top three layers are the same as the shallow seismic metamaterials and the bottom layer is bedrock. Different from the previous shallow seismic metamaterial configurations, we assume here that the bottom of the seismic metamaterial is fully clamped due to the strong constraint imposed by the bedrock. Fig. 4(a) and (b) show the phononic dispersion relations for homogeneous and layered seismic metamaterials with the same pile height, respectively. Similar to the shallow seismic metamaterial, an omnidirectional band gap still exists for the homogeneous seismic metamaterial configuration, and multiple partial band gaps also emerge for the layered seismic metamaterial. The eigenmodes (*A* and *B*) at the band edges for the former case suggest that Bragg scatterings are responsible for this omnidirectional band gap, while local resonances are responsible for the multiple partial band gaps, as evidenced by the

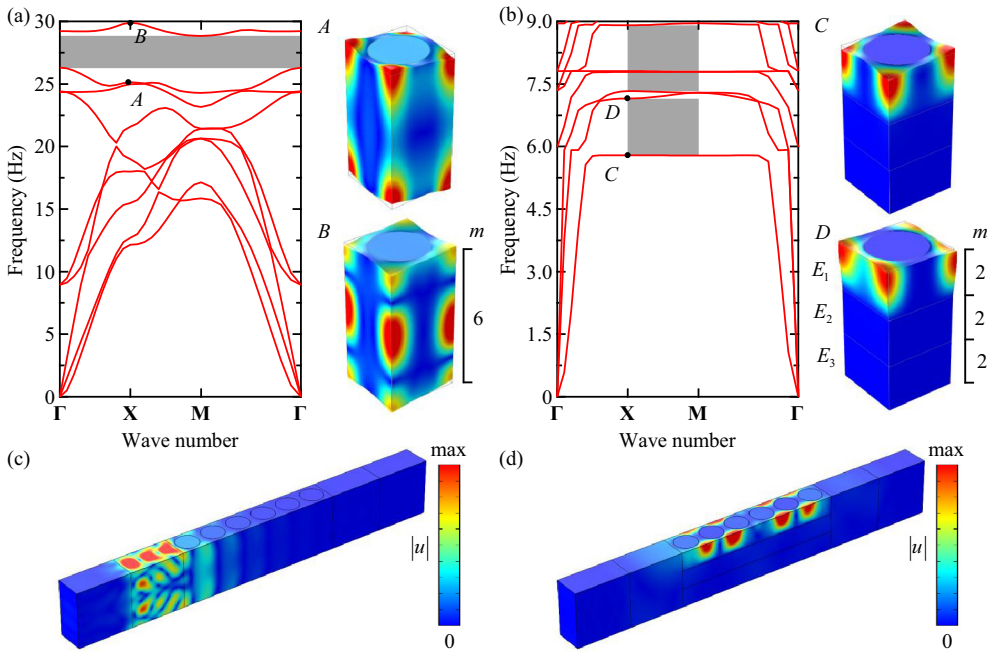

Fig. 3. Effect of the multi-layered feature on the vibration control of shallow layered seismic metamaterials. (a) Dispersion relation of the shallow seismic metamaterial with homogeneous soil. Here $h_1^I = 6$m, $a = 3$m, and $R = 1.2$ m. (b) Dispersion relation of the shallow layered seismic metamaterial. Here $h_1^{II} = h_2^{II} = h_3^{II} = 2$m, $a = 3$m, $R = 1.2$m, and $E_1 : E_2 : E_3 = 1 : 20 : 400$. The eigenmodes at high symmetry points are plotted. The gray shaded areas in (a) and (b) indicates the omnidirectional and partial band gaps, respectively. (c) Dynamic response of the shallow homogeneous seismic metamaterial at incident frequency f=27.6 Hz within the omnidirectional band gap. (d) Dynamic response of the shallow layered seismic metamaterial at incident frequency f=7 Hz within the first partial band gap. The color legends represent the displacement amplitude.

flat bands and confined wave energy in the soft layer (C and D). The most pronounced phenomenon in the dispersion relations for these two seismic metamaterials is the emergence of cut-off band gaps, as shown in the gray shaded areas in Fig. 4(a) and (b). Incident waves within these cut-off band gaps are fully suppressed (Fig. 4(c) and (d)). This remarkable feature arises from the artificially imposed boundary

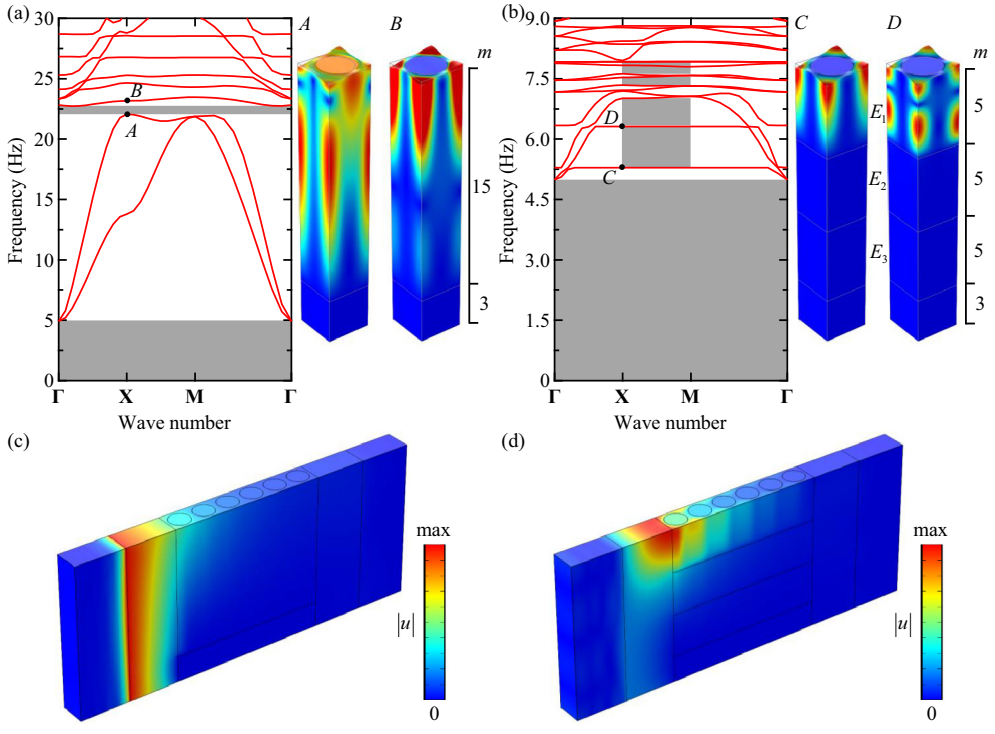

Fig. 4. Effect of the multi-layered feature on the vibration control of deep layered seismic metamaterials with a clamped boundary condition. (a) Dispersion relation of the deep seismic metamaterial with homogeneous soil. Here the height of the top homogeneous part and bedrock are 15 m and 3 m, respectively. (b) Dispersion relation of the deep layered seismic metamaterial. Here $h_1^{III} = h_2^{III} = h_3^{III} = 5$m, $h_4^{III} = 3$m, $a = 3$m, $R = 1.2$m, and $E_1 : E_2 : E_3 = 1 : 20 : 400$. The eigenmodes at high symmetry points are plotted. The gray shaded areas in (a) and (b) indicates the omnidirectional and partial band gaps, respectively. (c) Dynamic response of the homogenous seismic metamaterial at incident frequency f=2 Hz within the cutoff band gap. (d) Dynamic response of the layered seismic metamaterial at incident frequency f=4.5 Hz within the cutoff band gap. The color legends represent the displacement amplitude.

condition, which can be readily realized by drilling deep piles into bedrocks (when available or when artificially made). A similar phononic band gap property has been reported in structured soils modeled as a fully elastic layer periodically clamped to bedrock [21]. The cut-off band gaps reported in this work are generated by the strong constraint existing between pile and bedrock. In addition to this remarkable wave feature, we will show in the rest of the paper that the multi-layered soil feature of the proposed seismic metamaterials will enable us to tune elastic wave band gaps.

We have numerically demonstrated the surface wave attenuation capability of both shallow and deep layered seismic metamaterials. The shallow seismic configurations exhibit purely locally resonant band gaps, while the deep layered seismic metamaterials show both locally resonant and cut-off band gaps. For both cases, the wave energy can be confined in the softest layer due to the locally resonant phenomenon in the rationally designed seismic metamaterials. It should be pointed out that similar localized deformation modes have been reported in seismic metamaterials with single layered pillars [55] and phononic crystals composed of multi-layered pillars [56–58]. For example, in multi-layered pillared structures, the localized modes are generated at the interfaces between pillars and substrate, thereby coupling with surface waves and prohibiting their propagation. By contrast, the confined modes in the proposed seismic metamaterials can be easily tuned depending on the positions of the softest soil layer. Practically, this can be realized by engineering soil layering such as replacing the soil and using naturally existing multi-layered soil with stiffness contrast. In the following sections, we will evidence the robustness of the band gap properties for different combinations of soil layering and the possibility to tune these cut-off band gaps by varying the constraints between the bottom layer and the pile. Furthermore, the cost-effectiveness of the deep seismic metamaterials will be evaluated by investigating the effects of the pile volume fraction and pile shapes on the cut-off band gap size.

3.3. Effect of constraint between piles and bottom layer on vibration mitigation

We have shown that layered seismic metamaterials with deep concrete piles can attenuate surface wave with ultra-low frequencies, because of the strong constraint existing between piles and bedrock. In practice, depending on the interaction between bottom soil and piles, this strongly imposed boundary condition could be mitigated. To probe this, we study the effect of foundation stiffness ranging from 10^{10} to 10^{6} N/m·m^3 on the cut-off band gaps evolution. As shown in Fig. 5(a), a relatively weak constraint between soil and piles gives rise to a smaller cut-off band gap ranging between 0 and 0.97 Hz. With the increase of the foundation stiffness, the upper band of the cut-off band gap is enlarged to 4.92 Hz (Fig. 5(b)), which is about five times as the one with the softer foundation stiffness. The relation between foundation stiffness and cut-off band gap positions for both the homogeneous and the multi-layered seismic metamaterials are summarized in Fig. 5(c). Initially, the cut-off band gap size increases with the foundation stiffness and then becomes insensitive to the strong constraint. These quantitative analyses also imply that by tailoring the interaction between piles and the surrounding soil one can obtain tunable vibration band gaps, depending on the target vibration frequency ranges and the geological conditions. Notably, the evolution trends of these cut-off band gaps are almost the same for different combinations of soil layering, indicating the robustness of these band gaps and versatility of the proposed design.

3.4. Effect of pile volume fraction and pile shape on the vibration mitigation

The proposed deep seismic metamaterial composed of layered soil and circular concrete piles exhibits ultra-low frequency vibration control capability, which can be tuned by the foundation stiffness. In addition to altering the soil features, the volume fraction and shape of the pile are also critical in terms of the cost-effectiveness, because they are related to the use, volume, and logistics of the built environment. We first examine the effect of the deep pile volume fraction on the cut-off band gap evolution. As shown in Fig. 6(a), a cut-off band gap ranging from 0 to 2.5 Hz occurs for a relatively low volume fraction of concrete piles (20%). For a large volume fraction of concrete piles (70%), the cut-off band gap size is enlarged to 7 Hz (Fig. 6(b)). An almost linear relation between volume fraction and the cut-off band gap is summarized for both homogeneous and layered seismic metamaterials in Fig. 6(c). This analysis implies that by reducing the volume fraction of the concrete pile one could decrease the frequency range for vibration control.

To highlight the possibility that the proposed seismic metamaterials can reduce the use of concrete in the built environment, here we introduce hollow concrete piles and investigate the effect of the hollow pile radius on the cut-off band gap size. By gradually increasing the hollow pile radius from $r/R = 0.1$ to $r/R = 0.8 (R = 1.2\text{m})$, the cut-off band gap sizes are almost the same for the seismic metamaterials with

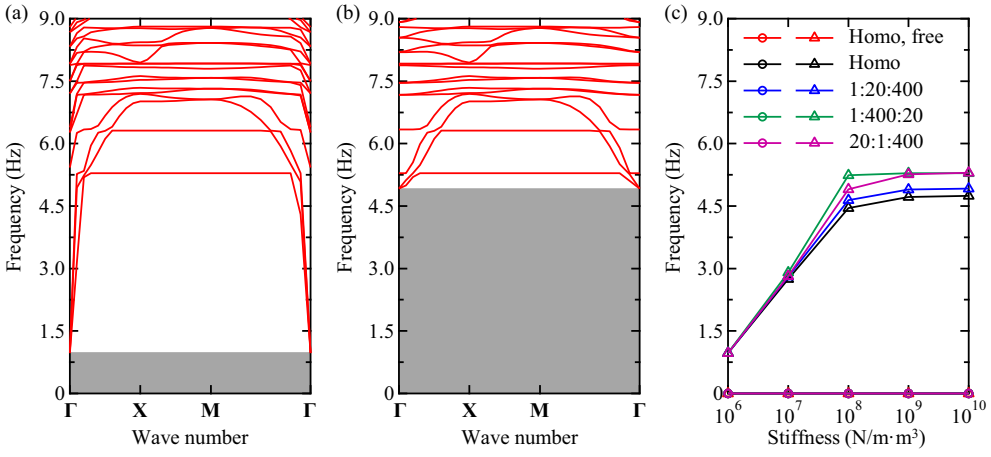

Fig. 5. Effect of the foundation stiffness on the cut-off band gap properties of deep layered seismic metamaterials. (a) The dispersion relation of the deep layered seismic metamaterial with a foundation stiffness of 10^6 N/m·m^3. (b) The dispersion relation of the deep layered seismic metamaterial with a foundation stiffness of 10^{10} N/m·m^3. The stiffness ratio among soil layers is $E_1 : E_2 : E_3 = 1 : 20 : 400$. (c) Effect of bottom layer stiffness on the evolution of cut-off band gap properties for different layered features and foundation stiffness. The ratio represents the stiffness contrast from the top to the bottom layer. Circles and triangles represent the frequencies of upper and lower edge limits of the omnidirectional band gaps, respectively. Here $h_1^{III} = h_2^{III} = h_3^{III} = 5\text{m}$, $h_4^{III} = 3\text{m}$, $a = 3\text{m}$, and $R = 1.2\text{m}$.

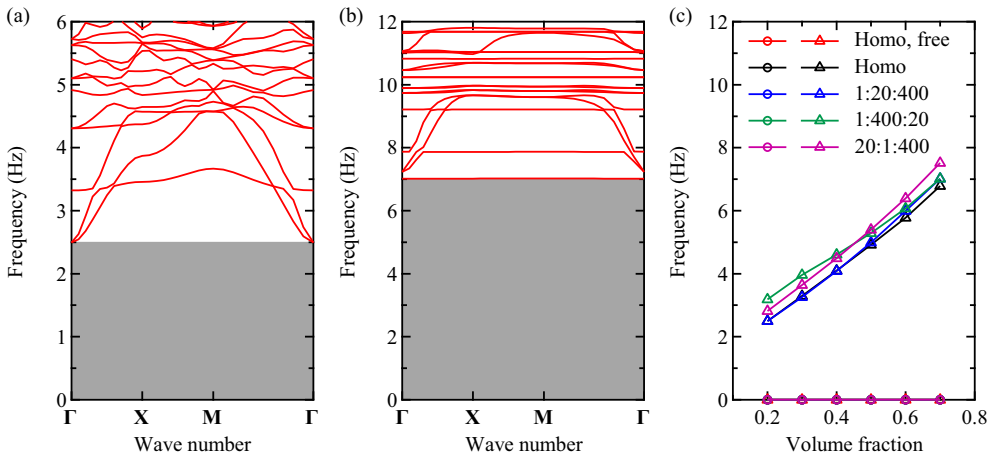

Fig. 6. Effect of pile volume fraction on the cut-off band gap properties of deep layered seismic metamaterials with a clamped boundary condition. (a) The dispersion relation of the deep layered seismic metamaterial with a pile volume fraction of 0.2. (b) Dispersion relation of the deep layered seismic metamaterial with a pile volume fraction of 0.7. The stiffness ratio among soil layers is $E_1 : E_2 : E_3 = 1 : 20 : 400$. (c) Effect of pile volume fraction on the cut-off band gap evolution for different layered features. The ratio represents the stiffness contrast from the top to the bottom layer. Circles and triangles represent the frequencies of upper and lower edge limits of the omnidirectional band gaps, respectively. Here $h_1^{III} = h_2^{III} = h_3^{III} = 5$m, $h_4^{III} = 3$m, and $a = 3$m.

different combinations of soil layering (Fig. 7). A further increase of the hollow radius leads to a negligible reduction on the cut-off band gaps size. Remarkably, the volume fraction of the concrete pile has been reduced from 50% to 9.4%; this clearly indicates that hollow concrete piles could be a cost-effective seismic metamaterial. It is interesting to note that the advantage of the hollow pile configurations has been numerically and experimentally reported in sound insulation and sound reflection measurements [59].

4. Conclusions

In summary, through an integrative experimental and numerical effort, we have demonstrated a new design methodology to create seismic metamaterials for low-frequency mechanical vibration mitigation. Our lab-scale experiments not only validated our computational models for wave propagation in 3D metamaterials, but also offer implications for subsequent large-scale and in-situ deployment of the proposed seismic metamaterials. The key aspect of this design of the seismic metamaterials is to consider the characteristics of multi-layered soils. Because of this multi-layered feature, the wave energy can be localized and steered out in the soft layer for shallow seismic metamaterials. For deep layered seismic metamaterials, in addition to the existence of omnidirectional band gaps, wide cut-off band gaps are observed, which offer unprecedented opportunities for ultra-low frequency vibration control. Furthermore, these cut-off band gaps can be tuned by tailoring the constraint between piles and the surrounding soil and the volume fraction of the solid piles. Quite importantly, we demonstrate that by introducing hollow piles into the multi-layered soil, one can achieve almost constant cut-off band gaps for the significantly-reduced volume fraction of the concrete pile. The design concept proposed here provides new insights into the development of seismic metamaterials to protect emergent structures from low-frequency vibrations and could find a wide range of engineering applications. For example, the shallow layered seismic metamaterials reported here can find applications in shallow foundations used in supporting various machinery. By using deep layered seismic metamaterials, one can protect deep structures such

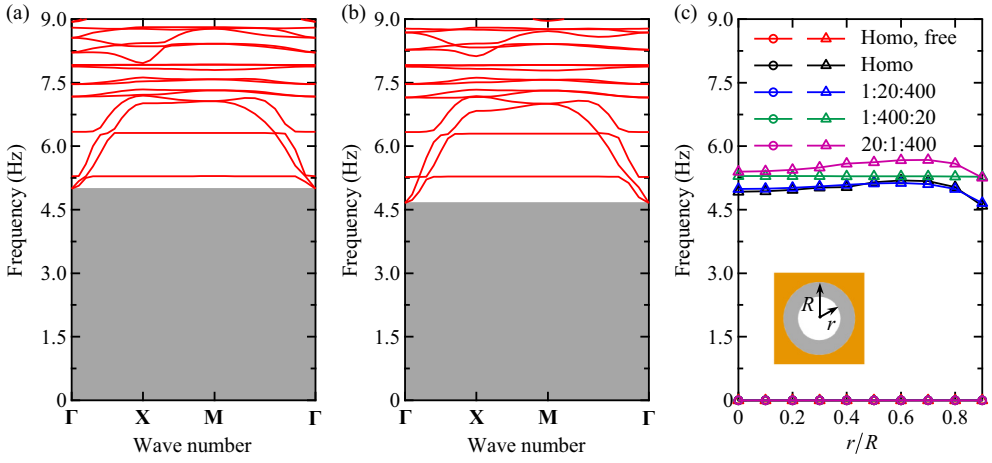

Fig. 7. Effect of the hollow pile shape on the cut-off band gap properties of deep layered seismic metamaterials with clamped boundary conditions. (a) The phononic dispersion relation of deep seismic metamaterial with a hollow pile radius of r/R=0.1. (b) The dispersion relation of deep seismic metamaterial with a hollow pile radius of r/R=0.9, where r and R are the inner and out radius of the hollow pile, respectively. The stiffness ratio among soil layers is $E_1 : E_2 : E_3 = 1 : 20 : 400$. (c) Effect of hollow pile radius on the band gap evolution for different layered features. The ratio represents the stiffness contrast from the top to the bottom layer. Circles and triangles represent the frequencies of upper and lower edge limits of the omnidirectional band gaps, respectively. Here $h_1^{III} = h_2^{III} = h_3^{III} = 5$m, $h_4^{III} = 3$m, $a = 3$m, and $R = 1.2$m.

as oil tank, nuclear power plants, fracking sites, and civil infrastructures from low-frequency surface waves from low-amplitude earthquakes. More investigation can be conducted to reveal the effect of soil visco-elasticity on the vibration mitigation capability of the proposed multi-layered seismic metamaterials.

Credit

Y. Chen performed the numerical simulations, F. Qian designed and conducted the experiments, F. Scarpa analyzed the data, L. Zuo and X. Zhuang supervised the research. All authors discussed the results and contributed to the final manuscript.

Acknowledgments

The Authors would like to thank the Editor and the anonymous Referees for the very constructive and useful comments. X Zhuang gratefully acknowledges financial support from the Peak Discipline Programme.

Competing interests

The authors declare no competing interests.

References

[1] P.W. Arnberg, O. Bennerhult, J.L. Eberhardt, Sleep disturbances caused by vibrations from heavy road traffic, J. Acoust. Soc. Am. 88 (3) (1990) 1486–1493.
[2] B. Dasgupta, D. Beskos, I. Vardoulakis, Vibration isolation using open or filled trenches part 2: 3-D homogeneous soil, Comput. Mech. 6 (2) (1990) 129–142.
[3] A. Israil, P. Banerjee, Two-dimensional transient wave-propagation problems by time-domain BEM, Int. J. Solids Struct. 26 (8) (1990) 851–864.
[4] R. Klein, H. Antes, D. Le Houédec, Efficient 3D modelling of vibration isolation by open trenches, Comput. Struct. 64 (1–4) (1997) 809–817.
[5] S. Kattis, D. Polyzos, D. Beskos, Vibration isolation by a row of piles using a 3-D frequency domain BEM, Int. J. Numer. Methods Eng. 46 (5) (1999) 713–728.
[6] G. Gao, et al., Three-dimensional analysis of rows of piles as passive barriers for ground vibration isolation, Soil Dyn. Earthq. Eng. 26 (11) (2006) 1015–1027.
[7] J. Avilés, F.J. Sánchez-Sesma, Foundation isolation from vibrations using piles as barriers, J. Eng. Mech. 114 (11) (1988) 1854–1870.
[8] M. Sun, et al., Analysis on multiple scattering by an arbitrary configuration of piles as barriers for vibration isolation, Soil Dyn. Earthq. Eng. 31 (3) (2011) 535–545.
[9] H. Takemiya, Field vibration mitigation by honeycomb WIB for pile foundations of a high-speed train viaduct, Soil Dyn. Earthq. Eng. 24 (1) (2004) 69–87.
[10] J. Vasseur, et al., Experimental and theoretical evidence for the existence of absolute acoustic band gaps in two-dimensional solid phononic crystals, Phys. Rev. Lett. 86 (14) (2001) 3012.
[11] A. Khelif, et al., Complete band gaps in two-dimensional phononic crystal slabs, Phys. Rev. E 74 (4) (2006) 046610.
[12] G. Wang, et al., Two-dimensional locally resonant phononic crystals with binary structures, Phys. Rev. Lett. 93 (15) (2004) 154302.
[13] Z. Liu, et al., Locally resonant sonic materials, science 289 (5485) (2000) 1734–1736.
[14] C. Sugino, et al., On the mechanism of bandgap formation in locally resonant finite elastic metamaterials, 120 (13) (2016) 134501.
[15] Y. Pennec, et al., Two-dimensional phononic crystals: examples and applications, Surf. Sci. Rep. 65 (8) (2010) 229–291.
[16] R.V. Craster, S. Guenneau, Acoustic Metamaterials: Negative Refraction, Imaging, Lensing and Cloaking, vol. 166, Springer Science & Business Media, 2012.
[17] P.A. Deymier, Acoustic Metamaterials and Phononic Crystals, vol. 173, Springer Science & Business Media, 2013.
[18] M. Miniaci, et al., Proof of concept for an ultrasensitive technique to detect and localize sources of elastic nonlinearity using phononic crystals, Phys. Rev. Lett. 118 (21) (2017) 214301.
[19] S. Castiñeira-Ibáñez, et al., Design, manufacture and characterization of an acoustic barrier made of multi-phenomena cylindrical scatterers arranged in a fractal-based geometry, Arch. Acoust. 37 (4) (2012) 455–462.
[20] G. Finocchio, et al., Seismic metamaterials based on isochronous mechanical oscillators, Appl. Phys. Lett. 104 (19) (2014), 191903.
[21] Y. Achaoui, et al., Clamped seismic metamaterials: ultra-low frequency stop bands, New J. Phys. 19 (6) (2017), 063022.
[22] A. Colombi, et al., Forests as a natural seismic metamaterial: Rayleigh wave bandgaps induced by local resonances, Sci. Rep. 6 (2016), 19238.
[23] A. Colombi, et al., A Seismic Metamaterial: The Resonant Metawedge. Scientific Reports, vol. 6, 2016 27717.
[24] M. Miniaci, et al., Large scale mechanical metamaterials as seismic shields, New J. Phys. 18 (8) (2016) 083041.
[25] S. Krödel, N. Thomé, C. Daraio, Wide band-gap seismic metastructures, Extreme Mech. Lett. 4 (2015) 111–117.
[26] A. Palermo, et al., Engineered metabarrier as shield from seismic surface waves, Sci. Rep. 6 (2016), 39356.
[27] O. Casablanca, et al., Seismic isolation of buildings using composite foundations based on metamaterials, J. Appl. Phys. 123 (17) (2018), 174903.
[28] Q. Du, et al., H-fractal seismic metamaterial with broadband low-frequency bandgaps, J. Phys. D. Appl. Phys. 51 (10) (2018), 105104.
[29] Z. Cheng, Z. Shi, Novel composite periodic structures with attenuation zones, Eng. Struct. 56 (2013) 1271–1282.
[30] Z. Shi, Z. Cheng, H. Xiang, Seismic isolation foundations with effective attenuation zones, Soil Dyn. Earthq. Eng. 57 (2014) 143–151.
[31] Z. Cheng, Z. Shi, Vibration attenuation properties of periodic rubber concrete panels, Constr. Build. Mater. 50 (2014) 257–265.
[32] G. Jia, Z. Shi, A new seismic isolation system and its feasibility study, Earthq. Eng. Eng. Vib. 9 (1) (2010) 75–82.
[33] J. Huang, Z. Shi, Application of periodic theory to rows of piles for horizontal vibration attenuation, Int. J. Geomech. 13 (2) (2011) 132–142.
[34] Z. Cheng, Z. Shi, Composite periodic foundation and its application for seismic isolation, Earthq. Eng. Struct. Dyn. 47 (4) (2018) 925–944.
[35] H. Xiang, et al., Periodic materials-based vibration attenuation in layered foundations: experimental validation, Smart Mater. Struct. 21 (11) (2012), 112003.
[36] S. Brûlé, et al., Experiments on seismic metamaterials: molding surface waves, Phys. Rev. Lett. 112 (13) (2014) 133901.
[37] Z. Cheng, et al., Locally resonant periodic structures with low-frequency band gaps, J. Appl. Phys. 114 (3) (2013), 033532.
[38] Basone, F., et al., Finite locally resonant metafoundations for the seismic protection of fuel storage tanks. Earthq. Eng. Struct. Dyn.
[39] G. Mylonakis, G. Gazetas, Settlement and additional internal forces of grouped piles in layered soil, Geotechnique 48 (1) (1998) 55–72.
[40] G. Militano, R. Rajapakse, Dynamic response of a pile in a multi-layered soil to transient torsional and axial loading, Geotechnique 49 (1) (1999) 91–109.
[41] M. Ashour, G. Norris, P. Pilling, Lateral loading of a pile in layered soil using the strain wedge model, J. Geotech. Geoenviron. 124 (4) (1998) 303–315.
[42] V. Laude, et al., Evanescent Bloch waves and the complex band structure of phononic crystals, Phys. Rev. B 80 (9) (2009) 092301.
[43] J.-C. Hsu, T.-T. Wu, Efficient formulation for band-structure calculations of two-dimensional phononic-crystal plates, Phys. Rev. B 74 (14) (2006), 144303.
[44] J. Mei, et al., Theory for elastic wave scattering by a two-dimensional periodical array of cylinders: an ideal approach for band-structure calculations, Phys. Rev. B 67 (24) (2003), 245107.
[45] A. Stock, D. Hannantt, R. Williams, The Effect of Aggregate Concentration Upon the Strength and Modulus of Elasticity of Concrete, 31(109), 1979 225–234.
[46] L. Bowles, Foundation Analysis and Design, McGraw-hill, 1996.
[47] A. Gómez-León, G. Platero, Floquet-Bloch theory and topology in periodically driven lattices, Phys. Rev. Lett. 110 (20) (2013) 200403.
[48] F. Moser, L.J. Jacobs, J. Qu, Modeling elastic wave propagation in waveguides with the finite element method, Ndt E Int. 32 (4) (1999) 225–234.
[49] L. De Marchi, A. Marzani, M. Miniaci, A dispersion compensation procedure to extend pulse-echo defects location to irregular waveguides, NDT E Int. 54 (2013) 115–122.
[50] T.-T. Wu, Z.-G. Huang, S. Lin, Surface and Bulk Acoustic Waves in Two-Dimensional Phononic Crystal Consisting of Materials with General Anisotropy, 69(9), 2004 094301.
[51] Y. Achaoui, et al., Experimental observation of locally-resonant and Bragg band gaps for surface guided waves in a phononic crystal of pillars, Phys. Rev. B 83 (10) (2011), 104201.
[52] M. Molerón, et al., Sound propagation in periodic urban areas, J. Appl. Phys. 111 (11) (2012), 114906.
[53] Y. Achaoui, et al., Experimental Observation of Locally-Resonant and Bragg Band Gaps for Surface Guided Waves in a Phononic Crystal of Pillars, 83(10), 2011 104201.
[54] Y. Chen, L. Wang, Isolation of surface wave-induced vibration using periodically modulated piles, Int. J. Appl. Mech. 6 (04) (2014), 1450042.
[55] Y. Zeng, et al., Low-Frequency Broadband Seismic Metamaterial Using I-Shaped Pillars in a Half-Space, 123(21), 2018 214901.
[56] M. Oudich, et al., Rayleigh Waves in Phononic Crystal Made of Multilayered Pillars: Confined Modes, Fano Resonances, and Acoustically Induced Transparency, vol. 9 (3), 2018 034013.
[57] M. Oudich, et al., Phononic Crystal Made of Multilayered Ridges on a Substrate for Rayleigh Waves Manipulation, vol. 7(12), 2017 372.
[58] C. Lim, J.J.E.S. Reddy, Built-up Structural Steel Sections as Seismic Metamaterials for Surface Wave Attenuation with Low Frequency Wide Bandgap in Layered Soil Medium, vol. 188, 2019 440–451.
[59] F. Morandi, et al., Standardised acoustic characterisation of sonic crystals noise barriers: sound insulation and reflection properties, Appl. Acoust. 114 (2016) 294–306.